Dynamics of Solar and Stellar Convection Zones and Atmospheres
Proceedings IAU Symposium No. 365, 2024
A. V. Getling & L. L. Kitchatinov, eds.
doi:10.1017/S1743921324000218

Flux emergence simulation and coronal response at ephemeral region scale

Zi–Fan Wang[1] **and R. H. Cameron**[2]

[1]National Astronomical Observatories, Chinese Academy of Sciences, Beijing, China
email: zfwang@nao.cas.cn

[2]Max Plank Institute for Solar System Research, Goettingen, Germany

Abstract. Flux emergence at different spatial scales and with different amounts of flux has been studied using radiative magnetohydrodynamics (rMHD) simulations. We use the radiative MHD code MURaM to simulate the emergence of an untwisted magnetic flux tube of ephemeral region scale with a density nonuniformity into a background atmosphere with a small unipolar open field. We find that the tube rises to the photosphere, forming complex loop structures seen in synthetic Atmospheric Imaging Assembly(AIA) 171 Å images. The atmosphere reaches $10^5 K$ at $3Mm$ above the surface. Our simulation provides a reference example of a less twisted ephemeral region emergence and the atmospheric response.

Keywords. Solar ephemeral region, Flux emergence

1. Introduction

The emergence of ephemeral regions is a kind of small-scale magnetic flux emergence between larger active regions and smaller intranetwork field emergences. They usually carry 10^{18} Mx to 10^{20} Mx flux and last at most 1-2 days (Harvey & Martin 1973; Hagenaar 2001). They tend to be important for flux emergence research, because they are related to both larger and smaller scale emergence in terms of physical mechanisms (Wilson et al. 1988; Illarionov et al. 2015), and play a part in the evolution of network fields (Hagenaar et al. 2003; van Driel–Gesztelyi & Green 2015). Being shorter lived, smaller in size and larger in number, ephemeral regions are good objects to study the whole process of emergence and proceeding evolution.

Previous magnetohydrodynamic (MHD) simulations of flux tube emergence show that a twist component of a magnetic flux tube is important for it to result in a successful flux emergence, because the twist can counteract deformation and fragmentation that will prevent the emergence of untwisted tubes (Schuessler 1979; Longcope et al. 1996; Moreno–Insertis & Emonet 1996; Krall et al. 1998). However, some observations suggests that flux tubes may not be twisted enough for successful emergence (Fan 2008). Hence, we try to examine the possible means of the emergence of a non-twisted tube.

In this proceeding we use numerical simulations to investigate the emergence of an ephemeral region. We consider the extreme case, introducing a non-twisted flux tube. We introduce a density nonuniformity, so that the tube is more buoyant in a part of it, and lead to its rise before complete fragmentation. We observe its emergence and the corresponding response in the corona, especially the temperature evolution.

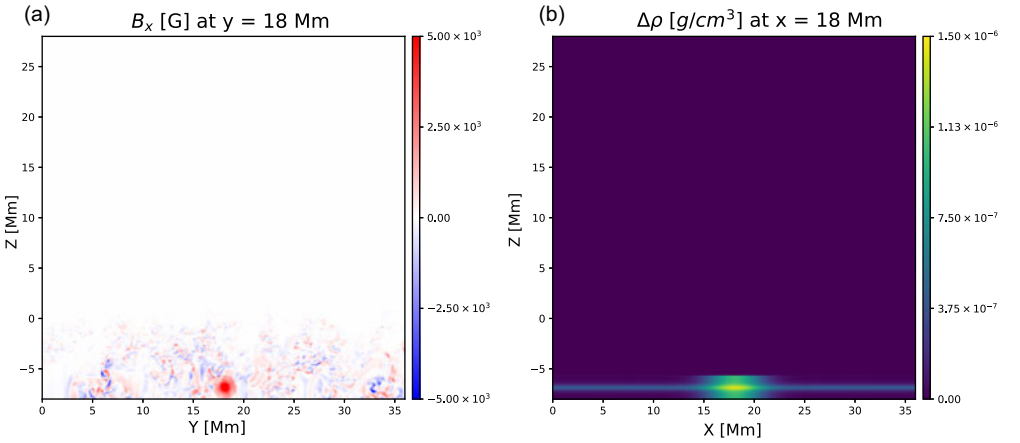

Figure 1. Initial conditions of the flux tube. Panels (a) shows B_x of an xz-slice at $y = 18$ Mm. Panel (b) shows the density decrease of introducing the tube $\Delta\rho = \rho - \rho_0$. Note that the uppermost part of the simulation domain is not presented here for convenience.

2. Methods

We use the radiative MHD code MURaM (Vögler et al. 2005; Rempel et al. 2009; Rempel 2017) to simulate the flux tube emergence and evolution. We use a 36 Mm × 36 Mm × 45 Mm Cartesian domain, with the third direction being vertical. The spatial resolution is 30 km for the vertical direction and 90 Mm for the horizontal directions, which is similar to previous simulations of active region evolution (e.g. Cheung et al. 2010; Rempel 2012; Chen et al. 2017). The boundaries of the two horizontal directions are periodic, while the upper boundary allows outflows. The photosphere where the optical depth τ is 1 is set to be 8 Mm above the bottom boundary, and is denoted as $z = 0$ Mm. A 5 G uniform magnetic field was added to the box, and is evolved until the magnetic energy reaches a statistically steady value.

We introduce a non-twisted magnetic flux tube near the bottom of the simulation domain. As shown in Figure 1 (a), the tube is parallel to the horizontal x-axis. The total flux is 1×10^{20} Mx, which is close to the flux of an ephemeral region (Harvey & Martin 1973). We then introduce a density nonuniformity to the tube, decreasing the density of part of the tube, in order to make the part rise faster. The location of the more buoyant part does not affect the results considering the periodic boundary conditions. The density nonuniformity follows a Gaussian function along the tube direction, as shown in Figure 1 (b).

We then simulate and examine the rise, emergence, and influence to the atmosphere of the flux tube. We examine the temperature, magnetic field, and the Poynting vector from the simulation. We also produce synthetic AIA images using the temperature response function from Lemen *et al.* (2012), and Boerner et al. (2012), as well as the optically-thin loss term in the corona of the MURaM model extension by Rempel (2017).

3. Results

The flux tube is simulated for 8 hours. It rises to the surface and emergence, forming loop structures and affects the properties in the atmosphere.

The time evolution of temperature in the layers of atmosphere is in agreement with the evolution of the surface field and synthetic AIA 171 Å images, and can be used to verify different periods of the simulation. As shown in Figure 2 and Figure 3, at around $t = 1.90$ hours, the temperature in the atmosphere is beginning to rise, and the emerging

https://doi.org/10.1017/S1743921324000218 Published online by Cambridge University Press

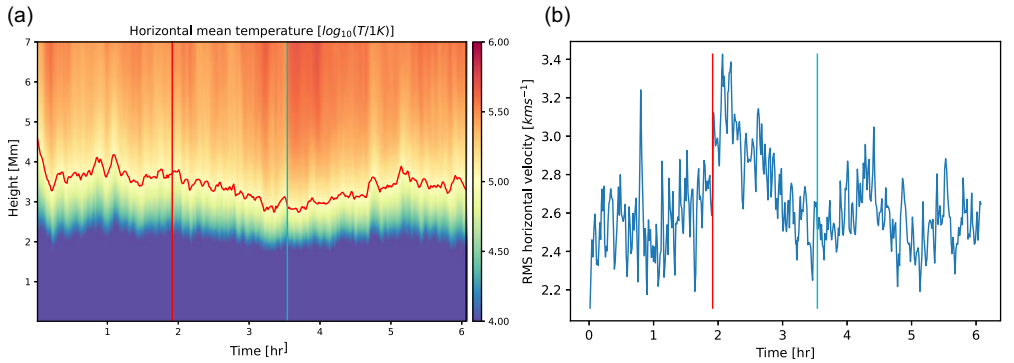

Figure 2. Time evolution of general properties during the flux emergence. Panel (a) shows the horizontally averaged temperature as a function of time and height above the photosphere. The red curve in panel (c) marks the height where the temperature is 10^5 K. Panel (b) shows the time evolution of root mean squared horizontal velocity ($v_{z,rms}$) in magnetic elements at the photosphere (at the average height of the $\tau = 1$ surface). The mean is taken over all pixels with vertical field larger in absolute value than 1×10^3 G. The red and cyan vertical lines represent 1.90 hours (red) and 3.53 hours (blue), respectively.

magnetic fields are observed at the photosphere surface. The AIA 171 Å images does not show complex structures compared to later time periods yet. After $t = 1.90$ hours, the temperature rise in the atmosphere is clearly shown, so the time period can be regarded as the main phase of the emergence. The $v_{h,rms}$ is the largest during the rapid rise of the surface flux, and falls quickly afterwards. At $t = 3.53$ hours, the photospheric vertical field at this time still possess a coherent negative polarity feature originating from the emergence, and the AIA 171 Å image shows complex structures in the atmosphere. After $t = 3.53$ hours, the transition region no longer moves downward, and begins to move back again, which marks the end of the main emergence process.

4. Discussions and conclusions

We have simulated the emergence of a flux tube at ephemeral region scale in a 3D domain with the radiative MHD model MURaM, covering it rise via magnetic buoyancy, photosphere surface emergence and atmosphere heating. During the simulation, the flux of the magnetic flux tube has emerged to the photosphere surface in the form of multiple bipoles. The emerged field generates loops reaching over 10 Mm in the atmosphere containing plasma above 10^6 K. The height of temperature reaching 10^5 K and 10^6 K during the emergence has lowered by 1 Mm in the atmosphere. After the peak, the temperature reverses to former condition as the movement of the surface field becomes less significant. The simulation describes a typical flux emergence in a partly fragmented form and with a limited effect in coronal response, which indicates the relationship between the influence to the atmosphere and the magnetic field configurations of ephemeral regions.

The flux tube we simulate is untwisted and with decreased density at its center. The emergence of twisted flux tube has been studied extensively, as an untwisted tube would distort and fragment during its rise (Schuessler 1979), disadvantageous to successful flux emergence. Twist field component keeps the tube from fragmentation and is important to flux emergence. However, our simulation shows that, for an untwisted tube, if the buoyancy at some part of it is large enough for it to rise before it fragments, a successful emergence is still possible. However, the emergence is fragmented and is limited in terms of heating in the atmosphere. How different properties of flux tubes affect atmospheric response differently is important in future study. Meanwhile, the emergence relies on the

https://doi.org/10.1017/S1743921324000218 Published online by Cambridge University Press

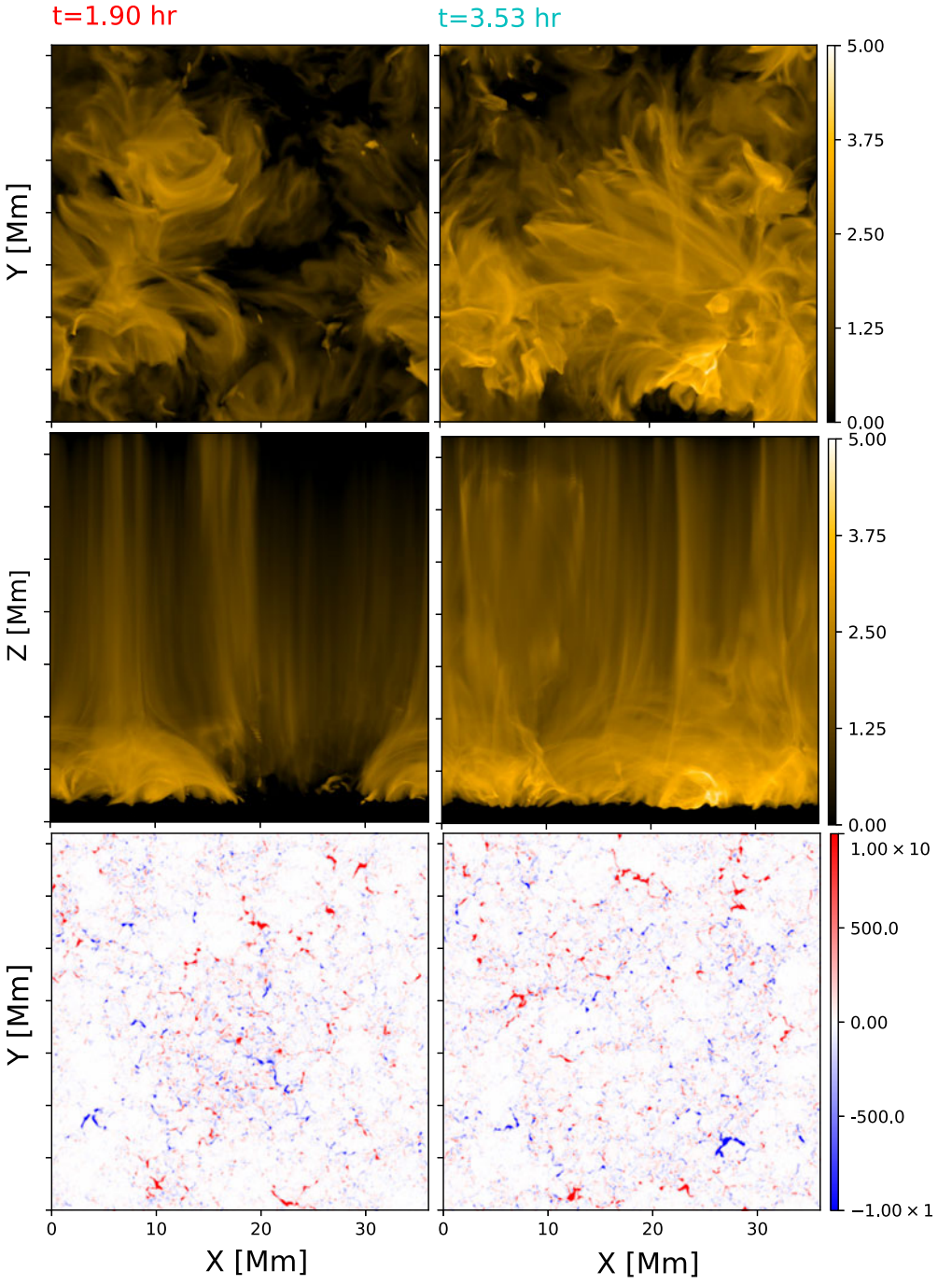

Figure 3. Synthetic 171 Å image and vertical photospheric magnetic field. The upper row shows the 171 Å image from the top, the middle row shows the 171 Å image from the yz plane, and the lower row shows the surface field. Columns 1 6 show the results at $t = 0.89$ hours, 1.90 hours, 2.52 hours, 3.15 hours, 3.53 hours, and 4.04 hours, respectively.

https://doi.org/10.1017/S1743921324000218 Published online by Cambridge University Press

density nonuniformity which may be caused by turbulent motions in the real sun, and is needed to be evaluated with more detail in observational study in the future.

References

Boerner, P., Edwards, C., Lemen, J., et al. 2012, *Solar Phys.*, 275, 41. doi:10.1007/s11207-011-9804-8

Chen, F., Rempel, M., & Fan, Y. 2017, *Astrophys. J.*, 846, 149. doi:10.3847/1538-4357/aa85a0

Cheung, M. C. M., Rempel, M., Title, A. M., et al. 2010, *Astrophys. J.*, 720, 233. doi:10.1088/0004-637X/720/1/233

Fan, Y. 2008, *Astrophys. J.*, 676, 680. doi:10.1086/527317

Hagenaar, H. J. 2001, *Astrophys. J.*, 555, 448. doi:10.1086/321448

Hagenaar, H. J., Schrijver, C. J., & Title, A. M. 2003, *Astrophys. J.*, 584, 1107. doi:10.1086/345792

Hale, G. E., Ellerman, F., Nicholson, S. B., et al. 1919, *Astrophys. J.*, 49, 153

Harvey, K. L. & Martin, S. F. 1973, *Solar Phys.*, 32, 389. doi:10.1007/BF00154951

Illarionov, E., Tlatov, A., & Sokoloff, D. 2015, *Solar Phys.*, 290, 351. doi:10.1007/s11207-014-0612-9

Krall, J., Chen, J., Santoro, R., et al. 1998, *Astrophys. J.*, 500, 992. doi:10.1086/305754

Lemen, J. R., Title, A. M., Akin, D. J., et al. 2012, *Solar Phys.*, 275, 17. doi:10.1007/s11207-011-9776-8

Longcope, D. W., Fisher, G. H., & Arendt, S. 1996, *Astrophys. J.*, 464, 999. doi:10.1086/177387

Moreno–Insertis, F. & Emonet, T. 1996, *Astrophys. J. Lett.*, 472, L53. doi:10.1086/310360

Rempel, M. 2012, *Astrophys. J.*, 750, 62. doi:10.1088/0004-637X/750/1/62

Rempel, M. 2017, *Astrophys. J.*, 834, 10. doi:10.3847/1538-4357/834/1/10

Rempel, M., Schüssler, M., & Knölker, M. 2009, *Astrophys. J.*, 691, 640. doi:10.1088/0004-637X/691/1/640

Schuessler, M. 1979, *Astron. Astrophys.*, 71, 79

van Driel–Gesztelyi, L., & Green, L. M. 2015, Living Reviews in Solar Physics, 12, 1

Vögler, A., Shelyag, S., Schüssler, M., et al. 2005, *Astron. Astrophys.*, 429, 335. doi:10.1051/0004-6361:20041507

Wilson, P. R., Altrocki, R. C., Harvey, K. L., et al. 1988, *Nature*, 333, 748. doi:10.1038/333748a0